Mehran University Research Journal of Engineering and Technology

https://doi.org/10.22581/muet1982.3372

2025, 44(1) 144-151

Synthesis and release profile of ibuprofen-loaded zein and gelatin nanofiber scaffolds for potential transdermal application in burn wound treatment

Umaima Saleem [a], Murk Saleem [b, *], Abdul Wahab Memon [a], Mehwish Shahzad [c], Murk Rehman [b], Farooq Ahmed [a], Zeeshan Khatri [a]

[a] *Department of Textile Engineering, Mehran University of Engineering and Technology, Jamshoro, Pakistan*

[b] *Institute of Biomedical Engineering and Technology, Liaquat University of Medical and Health Sciences, Jamshoro, Pakistan*

[c] *Department of Chemistry, Istanbul Technical University, Istanbul, Turkey*

[*] Corresponding author: Murk Saleem, Email: murk.saleem@lumhs.edu.pk

Received: 14 September 2024, Accepted: 26 December 2024, Published: 01 January 2025

K E Y W O R D S

Drug delivery

Antimicrobial

Electrospinning

Nanofiber mats

Burn care

A B S T R A C T

An antimicrobial barrier may accelerate rehabilitation by facilitating the healing of living tissues affected by injuries caused by burning. Fibrous mats based on nanotechnology have been extensively researched for their potential as drug delivery systems. The fabrication of electrospun polymeric nanofibrous mats containing non-steroidal anti-inflammatory medications (NSAIDs) and antibacterial agents has been discussed in this article. Electrospinning has been employed to create nanofibrous mats from pure zein and pure gelatin, and their combined use with Ibuprofen, an NSAID. Due to the ability of these electrospun nanofibrous mats to control exudation, they keep the site dry and shield it from microbiological activity, which makes them a good option for wound healing. In addition to providing an antibacterial layer that promotes wound healing, the manufactured mats can also function as medicine transporters. This research article extensively addresses the drug release profile from the carrier nanofibrous mats and the characteristics of fiber mats using standard characterization techniques like Fourier-transform infrared spectroscopy (FTIR) and Scanning electron microscope (SEM). The resultant fiber mats' drug release kinematics are compared to the standard mathematical models (Korsmeyer-pappas and Higuchi. The cumulative drug percentage released from these mats consistently validated Higuchi's model, which exhibited diffusion-controlled super case-II transport (n>1). The results indicate that the Ibuprofen is efficiently loaded onto the nanofibers, with a uniform distribution of the drug throughout the fiber matrix and ensures that the drug is released in a controlled and sustained manner, promoting effective wound healing.

1. Introduction

The skin is regarded as the largest organ of the human body and is essential for various physiological activities, such as sensing, thermoregulation, protection, and metabolic processes [1, 2]. The skin is required to remain healthy and unharmed to be able to safeguard against infection, preserve fluid balance, and control temperature [3]. The skin's barrier gets weakened by burn injuries, which elevates the possibility of bacterial infection [4]. When it comes to curing burn wounds for those who have sustained severe or extensive ignites, antimicrobial efficacy should come foremost [5].

Several technological advances have been implemented recently for treating burn injuries, such as skin grafting [6-8] and bioprinting [9-11], which

facilitate the creation of tailored skin grafts by printing layers of skin cells over burned areas. These grafts can be customized to the patient's burned skin type, facilitating a more rapid and effective process of healing [12, 13]. Further developments include growth factor therapy [14] and stem cell therapy [15], which use implantable cells that are specifically designed to have regenerative qualities. Encourage tissue repair, minimize inflammation, and accelerate healing when applied to burn injuries. Furthermore, transdermal use of modified wound dressings provides an efficient means of treating burn injuries [16]. The most efficient, ergonomic, economical, and effective transdermal burn injury treatment is through employing nanofiber scaffolds [17]. These dressings can replicate the extracellular matrix of the skin, acting as a scaffold for the proliferation of new cells. Most notably, they have a better ability to transport medications or antimicrobial agents to lessen pain and aid in the healing of burn injuries-related infections [17, 18]. In a more advanced drug delivery system, these nanofiber scaffolds act as smart bandages, releasing medication in reaction to changes in the wound environment, such as pH and temperature, to ensure burn injuries receive the appropriate care at the appropriate time [19].

Many studies are currently being conducted, especially on the potential use of biocompatible nanoparticles as antibacterial agents to prevent wound infection [20-22]. Biocompatible antimicrobial treatments assist deter bacteria from attacking wounds and improve gaseous exchange by keeping the surrounding area wet [23, 24]. Eminent to notify here that the primary source of infection in open wounds is bacteria, as these open wounds provide an easy way for microorganisms to enter the body and cause harm. Once enter the body, these bacteria damage deep soft tissues and may induce fatal internal infections [25].

Employing antimicrobial compounds in biocompatible nanomaterial-based scaffolds establishes a barrier for wounds and may boost antimicrobial activity to encourage wound healing [26]. Electrospun biopolymeric nanofibers, which are presently being researched as useful materials for wound dressings, may serve as a source for curing burn injuries effectively [27-29]. Biodegradable and biocompatible plant-based polymers, like Zein, have been utilized to create a multitude of films for use in biomedical applications [28]. In the food sector, zein—essentially a protein derived from corn—is frequently utilized as a coating ingredient [30]. It has been taken into consideration for several uses, including food packaging, tissue engineering scaffolds, medication transporters, and drug delivery systems [31, 32]. Zein nanofibers can be readily developed and produced by adjusting variables such as voltage, tip-to-collector distance, and solution viscosity using a straightforward electrospinning procedure [33]. Another polymer with good hemostatic properties and high macrophage activation is gelatin. Gelatin is economical, useful, and convenient [34-36]. However, there are few limitations of using zein based nanofibers for drug delivery, including their poor mechanical properties, limited drug loading capacity, and potential for immunogenicity [37].

Wound healing is a complex process that involves inflammation, tissue repair, and remodeling. Nonsteroidal anti-inflammatory drugs, such as Ibuprofen have been extensively used to manage inflammation and associated pain in various medicinal conditions, including wound care. The use of Ibuprofen drug with the electrospun nanofibers inhibits anti-inflammatory, antioxidant, and angiogenic effects, which are essential for reducing inflammation, and tissue damage, and promoting tissue repair [38].

2. Material And Methods

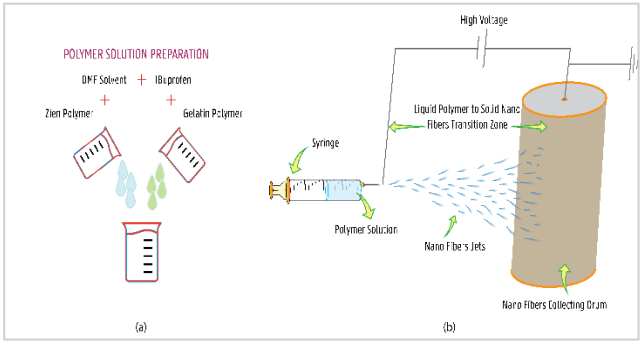

Fig. 1. Schematic Illustration Of (A) Polymer Preparation For Fabricating Zien And Gelatin Mixture-Based anofiber Scaffolds Loaded With Ibuprofen And (B) Their Electrospinning Process To Fabricate Respective Nanofiber Scaffolds Loaded

2.1 Materials

38 percent pure zein polymer, weight by weight (w/w), and 30 percent pure gelatin polymer (w/w) were obtained from Sigma-Aldrich - USA and used without further purification. Dimethylformamide - DMF was used as the solvent in combination with the zein polymer, while formic acid was used as the solvent for the gelatin polymer. Both the solvents were purchased from Daejung Chemicals and Metals Co. Ltd. Furthermore, to add antimicrobial characteristics to these polymers, Ibuprofen, purchased from Abbott Laboratories, Pakistan, was incorporated into each solution by 10% of the polymer's weight. Individual

polymer solution was stirred and mixed for three hours before their electrospinning was carried out.

2.2 Electrospinning

An electrospinning unit capable of generating high voltages of up to 100 kV was used to fabricate nanofiber scaffolds designed for burn wound treatment. Five different polymer solutions were prepared, and their corresponding nanofiber scaffolds were electrospun. The polymer solutions consisted of pure zein, zein with Ibuprofen, pure gelatin, gelatin with Ibuprofen, and a mixture of zein and gelatin with Ibuprofen. Each polymer solution was loaded into separate syringes fitted with capillary tips having an inner diameter of 0.6 mm. The negative electrode in a dedicated electrospinning process was connected to the collection drum where nanofibers were being collected. While positive electrode was submerged in the polymer solution through the copper wire attached to it. To collect the electrospun nanofibers, aluminum foil was wrapped carefully around the mandrel. The distance between the mandrel and the needle tip was maintained at 15 cm, with an angle of 10°. Nanofibers from each prepared solution were continuously deposited and collected on the surface of the drum. After that, the samples were stored for two days at room temperature to guarantee thorough drying of all specimens. Fig. 1 highlights the schematic approach through which (a) polymer solutions were prepared and (b) their respective electrospinning was performed.

2.3 Characterizations

The Zeiss Ultra Plus Field Emission Scanning Electron Microscope (SEM) was employed to assess gelatin and zein based nanofiber scaffolds for their surface morphology. This is essential because loading the medicine may change the surface attributes of the nanofiber scaffolds when incorporated into each polymer solution. All the SEM test specimens were carefully coated with gold, and later were subjected to the analysis at a voltage of 2kV. FT-IR spectra acquired with a Thermo Scientific iS10 FT-IR spectrometer were used to investigate the chemical composition of the nanofibers scaffolds. Further investigation was carried out with the analysis of the drug release behavior of zein and gelatin nanofiber scaffolds loaded with ibuprofen in a Phosphate-Buffered Saline (PBS) solution. The release behavior was examined using the ultraviolet-visible (UV-Vis) spectroscopy technique and was performed through a UV-Vis spectrophotometer. Later, by employing Image-J software, the mean diameter of the electrospun nanofibers loaded with Ibuprofen was calculated from SEM micrographs.

3. Results And Discussion

3.1 Morphology of Nanofibers

The SEM images were taken and analyzed for each nanofiber scaffold to examine their surface morphology. Therefore, electrospun nanofiber scaffolds from zein polymer (with and without Ibuprofen), gelatin polymer (with and without Ibuprofen), and combined ibuprofen-loaded zein-gelatin polymer-based nanofiber scaffolds were examined for their surface characteristics. Following this, the SEM image of the pure zein nanofiber scaffold and IBU-loaded zein nanofiber scaffold are illustrated in Fig. 2 (a) and (b) respectively.

By analyzing Fig. 2 (a), a randomly oriented network of dense nanofibers with uniform and smooth surfaces without any granularity can be observed. The nanofibers Come out with an average diameter of 200.5 nm. The network appears highly porous, and nanofibers intersect and overlap, creating a highly interconnected structure. Likewise, by examining Fig. 2 (b) indicating the SEM of zein polymer loaded with Ibuprofen drug, the nanofiber network appears to be dense but carries some lumps of dissolved Ibuprofen drug attached to the zein nanofibers. A notable change was observed in the average diameter of the Zein nanofibers when loaded with Ibuprofen drug which is 304 nm. The increase in the diameter of zein nanofibers is due to the extra layer of Ibuprofen.

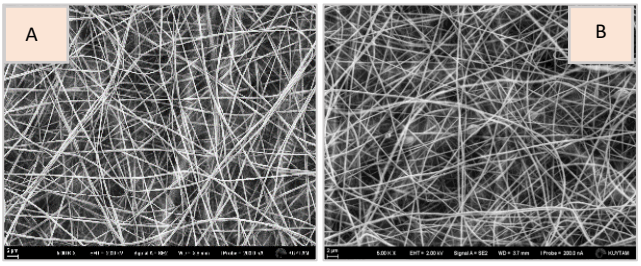

Fig. 2. SEM Images Of (A) Pure Zein And (B) Ibuprofen-Loaded Zein-Based Electro-Spun Nanofiber Scaffolds

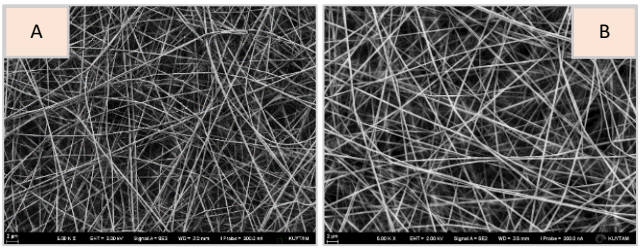

Fig. 3. SEM Images Of (A) Pure Gelatin And (B) Ibuprofen Loaded Gelatin Based Electro-Spun Nanofiber Scaffolds.

The SEM images based on pure gelatin nanofiber scaffold and IBU-loaded gelatin nanofiber scaffold are presented in Fig. 3 (a) and (b) respectively. Compared to the scaffold of zein-based nanofibers, the gelatin-based nanofiber network appears to be denser. The mean diameters of 190 nm and 275 nm were obtained for both the gelatin and Ibuprofen-loaded gelatin nanofibers. The denser network of gelatin-based nanofiber scaffolds may appear due to the slightly reduced diameter in their size compared to the zein-based nanofibers' diameter. More gelatin-based nanofibers can be accommodated per unit area than zein-based nanofibers. The SEM images indicate that the combined nanofibers retained their original morphology, with no physical changes apparent. The fibers remained intact, and no signs of degradation or aggregation were observed.

Fig. 4 illustrates the SEM image of IBU loaded on a mixture of zein and gelatin nanofibers. It appeared to have an average diameter of 493.77nm, the thickest among all other scaffold samples fabricated in this research.

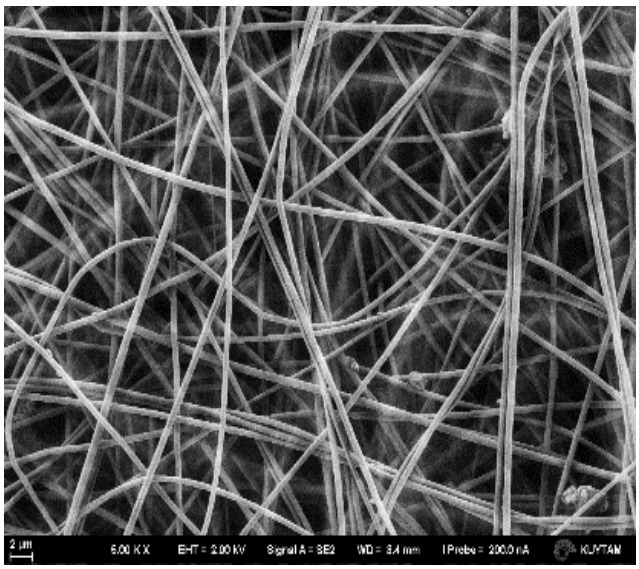

Fig.4. SEM Image Of Electro-Spun Nanofiber Scaffold Fabricated From A Mixture Of Zein, And Gelatin Nanofibers Loaded With Ibuprofen

3.2 Chemical Interaction Analysis

To observe the chemical reaction individual polymer itself and when interacted with Ibuprofen, FT-IR spectra tests were carried out and studied. Fig. 5 illustrates the FT-IR results of (a) pure zein nanofibers and zein nanofibers loaded with IBU, (b) pure gelatin nanofibers and gelatin nanofibers loaded with IBU, and (c) a mixture of zein and gelatin nanofibers and the same mixture of nanofibers loaded with IBU, respectively.

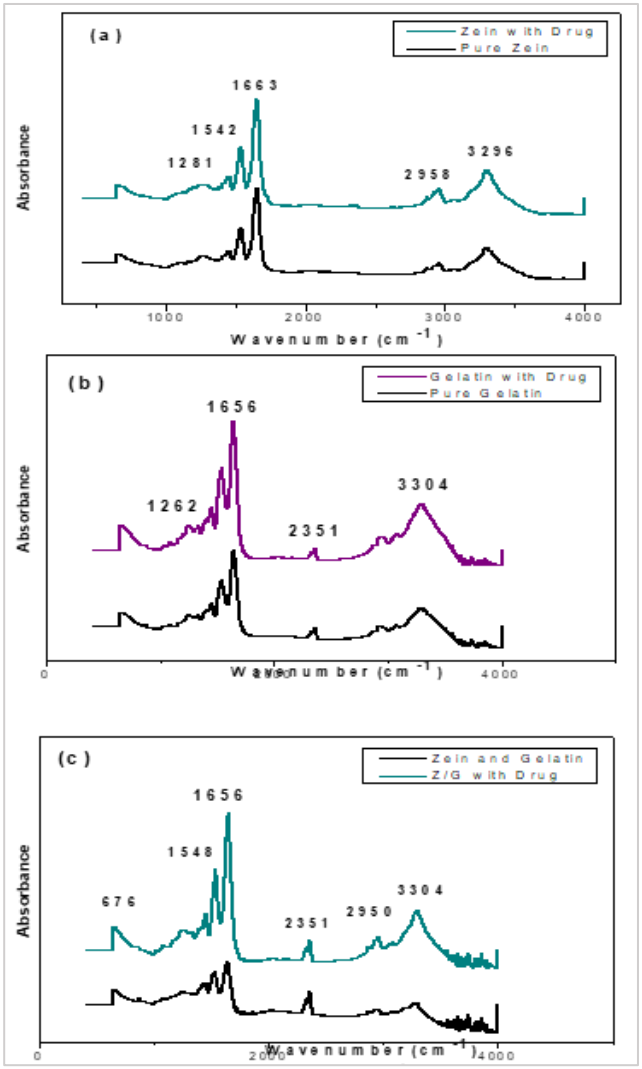

Fig.5. UV Spectroscopy Ofrolle (A) Pure Zein And IBU-Loaded Zein Nanofiber Scaffold (B) Pure Gelatin And IBU-Loaded Gelatin Nanofiber Scaffold (C) Zein/Gelatin And IBU-Loaded Zein/Gelatin Nanofiber Scaffold

The distinctive absorption band spanning 1281 cm^{-1}, 2958 cm^{-1}, 3296 cm^{-1}, and 1663 cm^{-1}, accordingly, is depicted in Fig. 5(a) and is associated with CN, CH, OH, and carbonyl stretching. The possible explanation for this may be due to the NH deformation, which may be the cause of the bands appearing at 1542 cm-1. The absorption bands seen in both pure zein and zein nanofiber loaded with IBU indicate that there is no adversarial response between IBU and the chemical makeup of pure zein. The distinct absorption band at 1262 cm^{-1}, 2351 cm^{-1}, and 3304 cm^{-1}, respectively, is associated with CN, NH_3, and NH stretching, as demonstrated in Fig. 5(b). A possible explanation for this may be due to NH2 deformation resulting in the bands at 1656 cm-1. Likewise, the absorption bands in both pure gelatin and gelatin nanofiber scaffolds loaded with IBU demonstrated that neither substance reacted negatively. subsequently, Fig. 5(c) illustrates the distinctive absorption band at 1656cm^{-1}. 2950cm^{-1}, 2950cm^{-1}, and 3304cm^{-1} correspond to the

carbonyl, NH_3, CH, and NH stretching respectively. It is experienced that C-O-H bending is the cause of the band at 676 cm^{-1}. The FT-IR spectra of zein and gelatin scaffold, as well as the IBU-loaded combined Zein/Gelatin scaffold, also show peaks at the identical bands with molecule stretching and bending. The peak at 1548cm^{-1} conforms to the NH deformation.

3.3 Release Profile of Resultant Nanofibers

The ultraviolet (UV)-visible spectrophotometer was calibrated using various IBU drug concentrations (150 ppm, 125 ppm, 100 ppm, 75 ppm, and 50 ppm) in PBS solution to examine the release behavior of IBU from artificial zein and gelatin nanofiber scaffolds. The IBU medication peaked at about ~264 nm. 30 milligrams of combined Zein/Gelatin nanofibrous scaffold loaded with IBU (containing 3.0 mg of medicine) was dissolved in 30 ml PBS at 37°C and vigorously swirled. Every five minutes, samples were examined using UV-visible spectroscopy, and fresh samples were added to the solution to ensure that the cumulative drug release was reflected in each one. Within two hours, the whole dose of IBU was freed from its nanofiber scaffold sheet. The pattern of drug released is adapted to pharmacokinetics models, such as Higuchi's model and Korsmeyer-Pappas to study the kinetics of drug release in vitro.

Higuchi`s model used to study drug release behavior is represented by Eq. (1).

$$Q = k_H t^{1/2} \quad \text{(Eq. 1)}$$

Q = Cumulative % of drug release

K_H = Higuchi`s constant

t = time in hours.

Plotting the collected data as a cumulative percentage of drug release (Q) against the square root of "t" (time) was conducted. Fig. 6 (a) depicts the drug release profile which is in trendline with a high coefficient of correlation indicating the cumulative drug release percentage. The pattern also illustrates that the released drug from the nanofibrous layer follows Higuchi's mode. A greater correlation coefficient indicates that a diffusion-controlled release mechanism was used to release the medication. It is crucial to confirm the type of diffusion that IBU release behavior is adhering to after examining the drug's diffusion-controlled release behavior from the nanofiber scaffold. The Korsmeyer–Pappas model was applied for that reason.

$$\frac{M_t}{M_\infty} = kt^n \quad \text{(Eq. 2)}$$

$M_t/M\infty$ = fraction of released drug

K_m= Structural and geometrical characteristics constant

t = time

n = release component

As seen in Fig. 6(b), the log of the cumulative percentage of medication released was plotted along log(t) to examine drug release kinetics.

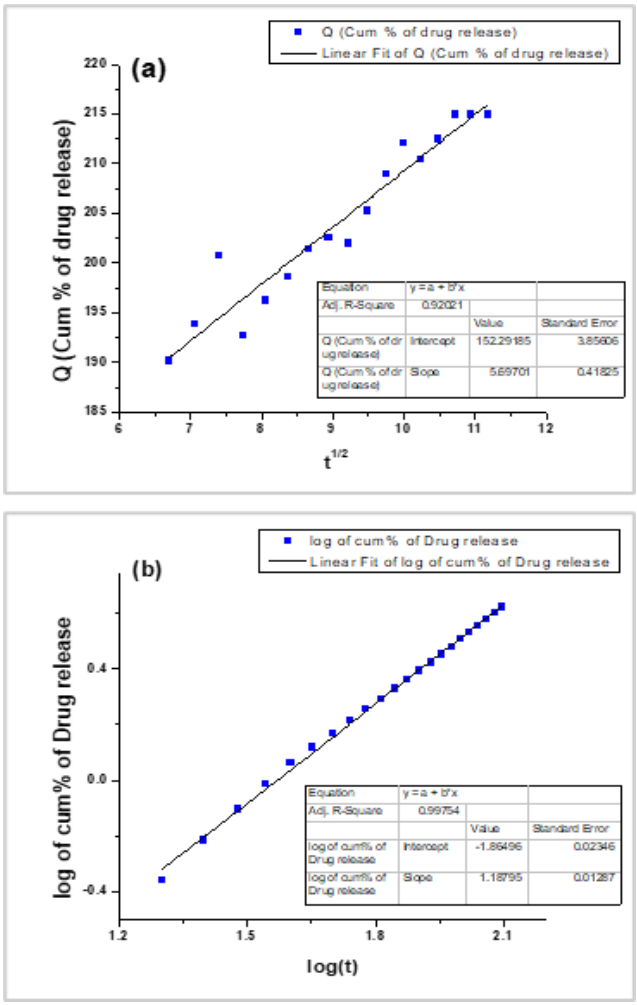

Fig. 6. Illustrates (a) Higuchi`s Model Fit, (b) Korsmeyer Pappa Model Fit

The value of "n" is used to describe the release method. The various drug release mechanisms listed in Table 1 are represented by the value of "n".

Table 1

Diffusion exponent and drug release mechanism [15-17]

Release Component (n)	Drug Release Mechanism
0.5	Fickian diffusion
0.5<n<1	Non-fickian or anomalous transport
1	Case-II transport
n>1	Super Case-II transport

Krosmayer Peppas modelling for this sample represents that the drug followed CASE-II transport as a value of n is 1.188, which represent diffusion is case-II transport shown in Table 2.

Table 2

Kinetic model`s characteristic summary

Korsmayer Peppas Model	Higuchi`s Kinetic Model
n= 1.188	KH= 5.697
Km = 0.0136	R2= 0.9252
R2= 0.9977	

Ibuprofen is methodically released from the fibrous layer following the drug model (Higuchi), with a correlation coefficient (r2= 0.9252) of 0.9252. Diffusion-controlled Super case II transport is in parallel to controlling the drug release from the system. As a result, the resulting nanofibrous scaffolds have a great deal of potential for use as antimicrobial fences that can release medications over time in burn sites. The higher loading rate of ibuprofen in nanofibers led to a faster release rate and higher bioavailability, which will accelerate the wound healing process. However, it is significant to note that the excessive use of the drug can lead to impaired wound healing and toxicity.

4. Conclusion

Fourier Transform Infrared spectroscopic images showed that zein and Gelatin are distinctively compatible with Ibuprofen. According to the peak representation of the drug and polymer, it was proved that both do not react oppositely with each other. Scanning electron microscopic images of zein and gelatin loaded with Ibuprofen were seen morphologically bead-free with a diameter of 493.7nm. However, the release of drugs from the polymers followed Higuchi`s drug release model with a coefficient correlation value of 0.9252. The Ibuprofen release from the polymer showed the diffusion of Super case-II transport. Therefore, the nanofibrous sheet has proved to have the capability to function as the antimicrobial barrier along with the ability to release drugs in burn wounds. It is expected from the findings suggested that increasing the loading rate of ibuprofen in nanofibers can enhance its efficacy in promoting wound healing.

5. References

[1] O. Forson, E. Ayanka, M. Olu-Taiwo, P. Pappoe-Ashong, and P. Ayeh-Kumi, “Bacterial infections in burn wound patients at a tertiary teaching hospital in Accra, Ghana”, Annals of burns and fire disasters, vol. 30, p. 116, 2017.

[2] G. Menon and A. Kligman, “Barrier functions of human skin: a holistic view”, Skin pharmacology and physiology, vol. 22, pp. 178-189, 2009.

[3] A. Shpichka, D. Butnaru, E. A. Bezrukov, R. B. Sukhanov, A. Atala, V. Burdukovskii, et al., “Skin tissue regeneration for burn injury”, Stem cell research & therapy, vol. 10, pp. 1-16, 2019.

[4] J. K. Plichta, C. J. Holmes, R. L. Gamelli, and K. A. Radek, “Local burn injury promotes defects in the epidermal lipid and antimicrobial peptide barriers in human autograft skin and burn margin: implications for burn wound healing and graft survival”, Journal of Burn Care & Research, vol. 38, pp. e212-e226, 2017.

[5] M. P. Rowan, L. C. Cancio, E. A. Elster, D. M. Burmeister, L. F. Rose, S. Natesan, et al., “Burn wound healing and treatment: review and advancements”, Critical care, vol. 19, pp. 1-12, 2015.

[6] D. K. Ozhathil, M. W. Tay, S. E. Wolf, and L. K. Branski, “A narrative review of the history of skin grafting in burn care”, Medicina, vol. 57, p. 380, 2021.

[7] F. Schlottmann, V. Bucan, P. M. Vogt, and N. Krezdorn, “A short history of skin grafting in burns: From the gold standard of autologous skin grafting to the possibilities of allogeneic skin grafting with immunomodulatory approaches”, Medicina, vol. 57, p. 225, 2021.

[8] H. Luze, S. P. Nischwitz, C. Smolle, R. Zrim, and L.-P. Kamolz, “The use of acellular fish skin grafts in burn wound management—a systematic review”, Medicina, vol. 58, p. 912, 2022.

[9] M. Varkey, D. O. Visscher, P. P. Van Zuijlen, A. Atala, and J. J. Yoo, “Skin bioprinting: the future of burn wound reconstruction?”, Burns & trauma, vol. 7, 2019.

[10] Y. Wu, T. Liang, Y. Hu, S. Jiang, Y. Luo, C. Liu, et al., “3D bioprinting of integral ADSCs-NO hydrogel scaffolds to promote severe burn wound healing”, Regenerative biomaterials, vol. 8, p. rbab014, 2021.

[11] P. He, J. Zhao, J. Zhang, B. Li, Z. Gou, M. Gou, et al., “Bioprinting of skin constructs for wound healing”, Burns & trauma, vol. 6, 2018.

[12] N. Brusselaers, A. Pirayesh, H. Hoeksema, C. D. Richters, J. Verbelen, H. Beele, et al., “Skin replacement in burn wounds”, Journal of

Trauma and Acute Care Surgery, vol. 68, pp. 490-501, 2010.

[13] M. Singh, K. Nuutila, K. Collins, and A. Huang, "Evolution of skin grafting for treatment of burns: Reverdin pinch grafting to Tanner mesh grafting and beyond", Burns, vol. 43, pp. 1149-1154, 2017.

[14] C.-m. Han, B. Cheng, P. Wu, and W. G. o. G. F. G. o. B. o. C. B. Association, "Clinical guideline on topical growth factors for skin wounds", Burns & Trauma, vol. 8, p. tkaa035, 2020.

[15] M. Wang, X. Xu, X. Lei, J. Tan, and H. Xie, "Mesenchymal stem cell-based therapy for burn wound healing", Burns & trauma, vol. 9, p. tkab002, 2021.

[16] A. Oryan, E. Alemzadeh, and A. Moshiri, "Burn wound healing: present concepts, treatment strategies and future directions", Journal of wound care, vol. 26, pp. 5-19, 2017.

[17] N. Talebi, D. Lopes, J. Lopes, A. Macário-Soares, A. K. Dan, R. Ghanbari, et al., "Natural polymeric nanofibers in transdermal drug delivery", Applied Materials Today, vol. 30, p. 101726, 2023.

[18] L. Kumar, S. Verma, K. Joshi, P. Utreja, and S. Sharma, "Nanofiber as a novel vehicle for transdermal delivery of therapeutic agents: challenges and opportunities", Future Journal of Pharmaceutical Sciences, vol. 7, p. 175, 2021.

[19] Ziauddin, T. Hussain, A. Nazir, U. Mahmood, M. Hameed, S. Ramakrishna, et al., "Nanoengineered therapeutic scaffolds for burn wound management", Current pharmaceutical biotechnology, vol. 23, pp. 1417-1435, 2022.

[20] T. Baygar, N. Sarac, A. Ugur, and I. R. Karaca, "Antimicrobial characteristics and biocompatibility of the surgical sutures coated with biosynthesized silver nanoparticles", Bioorganic chemistry, vol. 86, pp. 254-258, 2019.

[21] M. Ozdal and S. Gurkok, "Recent advances in nanoparticles as antibacterial agent", ADMET and DMPK, vol. 10, pp. 115-129, 2022.

[22] S. Hu, X. Cai, X. Qu, B. Yu, C. Yan, J. Yang, et al., "Preparation of biocompatible wound dressings with long-term antimicrobial activity through covalent bonding of antibiotic agents to natural polymers", International journal of biological macromolecules, vol. 123, pp. 1320-1330, 2019.

[23] R. Jayakumar, M. Prabaharan, P. S. Kumar, S. Nair, and H. Tamura, "Biomaterials based on chitin and chitosan in wound dressing applications", Biotechnology advances, vol. 29, pp. 322-337, 2011.

[24] A. R. Unnithan, G. Gnanasekaran, Y. Sathishkumar, Y. S. Lee, and C. S. Kim, "Electrospun antibacterial polyurethane–cellulose acetate–zein composite mats for wound dressing", Carbohydrate polymers, vol. 102, pp. 884-892, 2014.

[25] P. Sudheesh Kumar, V.-K. Lakshmanan, T. Anilkumar, C. Ramya, P. Reshmi, A. Unnikrishnan, et al., "Flexible and microporous chitosan hydrogel/nano ZnO composite bandages for wound dressing: in vitro and in vivo evaluation", ACS applied materials & interfaces, vol. 4, pp. 2618-2629, 2012.

[26] L. R. Lakshman, K. Shalumon, S. V. Nair, R. Jayakumar, and S. Nair, "Preparation of silver nanoparticles incorporated electrospun polyurethane nano-fibrous mat for wound dressing", Journal of Macromolecular Science, Part A: Pure and Applied Chemistry, vol. 47, pp. 1012-1018, 2010.

[27] K. N. Kontogiannopoulos, A. N. Assimopoulou, I. Tsivintzelis, C. Panayiotou, and V. P. Papageorgiou, "Electrospun fiber mats containing shikonin and derivatives with potential biomedical applications", International journal of pharmaceutics, vol. 409, pp. 216-228, 2011.

[28] J. Lin, C. Li, Y. Zhao, J. Hu, and L.-M. Zhang, "Co-electrospun nanofibrous membranes of collagen and zein for wound healing", ACS applied materials & interfaces, vol. 4, pp. 1050-1057, 2012.

[29] U. Dashdorj, M. K. Reyes, A. R. Unnithan, A. P. Tiwari, B. Tumurbaatar, C. H. Park, et al., "Fabrication and characterization of electrospun zein/Ag nanocomposite mats for wound dressing applications", International journal of biological macromolecules, vol. 80, pp. 1-7, 2015.

[30] B. Kong and Y. L. Xiong, "Antioxidant activity of zein hydrolysates in a liposome system and the possible mode of action", Journal of agricultural and food chemistry, vol. 54, pp. 6059-6068, 2006.

[31] X. Liu, Q. Sun, H. Wang, L. Zhang, and J.-Y. Wang, "Microspheres of corn protein, zein, for

an ivermectin drug delivery system", Biomaterials, vol. 26, pp. 109-115, 2005.

[32] S. Gong, H. Wang, Q. Sun, S.-T. Xue, and J.-Y. Wang, "Mechanical properties and in vitro biocompatibility of porous zein scaffolds", Biomaterials, vol. 27, pp. 3793-3799, 2006.

[33] K. Kanjanapongkul, S. Wongsasulak, and T. Yoovidhya, "Investigation and prevention of clogging during electrospinning of zein solution", Journal of applied polymer science, vol. 118, pp. 1821-1829, 2010.

[34] A. Arun, P. Malrautu, A. Laha, and S. Ramakrishna, "Gelatin nanofibers in drug delivery systems and tissue engineering", Engineered Science, vol. 16, pp. 71-81, 2021.

[35] H. R. El-Seedi, N. S. Said, N. Yosri, H. B. Hawash, D. M. El-Sherif, M. Abouzid, et al., "Gelatin nanofibers: Recent insights in synthesis, bio-medical applications and limitations", Heliyon, vol. 9, 2023.

[36] Z.-M. Huang, Y. Zhang, S. Ramakrishna, and C. Lim, "Electrospinning and mechanical characterization of gelatin nanofibers", Polymer, vol. 45, pp. 5361-5368, 2004.

[37] Y. Zhang, L. Cui, Y. Chen, H. Zhang, J. Zhong, Y. Sun, et al., "Zein-based nanofibres for drug delivery: classes and current applications", Current Pharmaceutical Design, vol. 21, pp. 3199-3207, 2015.

[38] P. Price, K. Fogh, C. Glynn, D. L. Krasner, J. Osterbrink, and R. G. Sibbald, "Why combine a foam dressing with ibuprofen for wound pain and moist wound healing?", International Wound Journal, vol. 4, p. 1, 2007.

